AIP | Applied Physics Letters

Ferroelectric memristor based on Pt/BiFeO3/Nb-doped SrTiO3 heterostructure

Zhongqiang Hu, Qian Li, Meiya Li, Qiangwen Wang, Yongdan Zhu et al.

Citation: Appl. Phys. Lett. **102**, 102901 (2013); doi: 10.1063/1.4795145
View online: http://dx.doi.org/10.1063/1.4795145
View Table of Contents: http://apl.aip.org/resource/1/APPLAB/v102/i10
Published by the American Institute of Physics.

Ferroelectric memristor based on Pt/$BiFeO_3$/Nb-doped $SrTiO_3$ heterostructure

Zhongqiang Hu,[1,a)] Qian Li,[2] Meiya Li,[1,b)] Qiangwen Wang,[1] Yongdan Zhu,[1] Xiaolian Liu,[1] Xingzhong Zhao,[1] Yun Liu,[2] and Shuxiang Dong[3]
[1]*School of Physics and Technology, and Key Laboratory of Artificial Micro/Nano Structures of Ministry of Education, Wuhan University, Wuhan 430072, People's Republic of China*
[2]*Research School of Chemistry, The Australian National University, ACT 0200, Australia*
[3]*Department of Materials Science and Engineering, College of Engineering, Peking University, Beijing 100871, People's Republic of China*

(Received 27 November 2012; accepted 27 February 2013; published online 11 March 2013)

We report a continuously tunable resistive switching behavior in Pt/$BiFeO_3$/Nb-doped $SrTiO_3$ heterostructure for ferroelectric memristor application. The resistance of this memristor can be tuned up to 5×10^5% by applying voltage pulses at room temperature, which exhibits excellent retention and anti-fatigue characteristics. The observed memristive behavior is attributed to the modulation effect of the ferroelectric polarization reversal on the width of depletion region and the height of potential barrier of the *p-n* junction formed at the $BiFeO_3$/Nb-doped $SrTiO_3$ interface. © *2013 American Institute of Physics*. [http://dx.doi.org/10.1063/1.4795145]

Resistive switching has been observed in capacitor-like structures consisting of ferroelectric thin films, in which the resistance can be reversibly switched between a high resistance state (HRS) and a low resistance state (LRS) by applying voltages.[1,2] These two resistance states can be used in bistable memory devices. More importantly, continuously tunable resistors, i.e., memristors, have been recently demonstrated in ferroelectric tunnel junctions.[3,4] The memristors, also known as the fourth fundamental circuit element in addition to resistors, capacitors, and inductors,[5] have potential applications in high-density multilevel nonvolatile memories and adaptive networks that require synapse-like functions.[4]

Resistive switching behavior in multiferroic $BiFeO_3$ (BFO) has attracted considerable attention because it offers additional degrees of freedom for BFO-based multifunctional devices.[6–14] The observed resistive switching phenomena in BFO films appear to vary with the processing conditions and microstructures of the films, suggesting that several mechanisms may be involved. Possible mechanisms proposed by prior studies can be classified into two types: (i) conductive filament type.[6–8] During the electroforming process, local conductive paths consisted of oxygen vacancies or metallic filaments are formed in the insulating BFO matrix thus switching the device to LRS; the conductive filaments can be damaged by applying reverse voltages so that the device changes back to HRS. This filamentary resistive switching usually appears in capacitor-like structures with polycrystalline BFO films,[6–8] in which the forming and damage of filaments accompany with abrupt changes in electrical current. However, since chemical alterations such as local redox reactions or cation valence changes are involved in this mechanism, there are concerns about the reliability of such type of devices in terms of retention and endurance.[14,15] (ii) Ferroelectric polarization modulated interface type.[10–14] Generally, BFO films exhibit *p*-type conduction as a result of Bi loss.[11,14,16] Thus, a Schottky junction or a *p-n* junction may be formed at the metal/BFO interface or the BFO/*n*-type semiconductor interface, respectively. These junctions can be modulated by the ferroelectric polarization, which induces blocking or nonblocking interfaces for the transport of carriers and consequently the resistive switching behavior.[10–14] In contrast to that in a conventional heterostructure, the interfacial state in a ferroelectric semiconductor heterojunction can be gradually modified by the polarization reversal, which may give rise to a continuously tunable resistive switching behavior (i.e., memristive behavior).[3,4] Since the polarization reversal has a superior stability to that of a chemical alteration and is intrinsically fast,[17] the interfacial resistive switching is highly favorable to the newly emerging ferroelectric memristors.[3,4] However, with many reports focusing on the bistable resistive switching in BFO, the memristive behavior has not yet attracted enough attention.

In this letter, we report the memristive behavior in Pt/BFO/Nb-doped $SrTiO_3$ heterostructure with a continuous tunability up to 5×10^5%. It is also verified that the ferroelectric polarization enhances the reliability such as the retention and anti-fatigue characteristics. We attribute the observed memristive behavior to the ferroelectric polarization modulation of the depletion width and the barrier height at the BFO/Nb-doped $SrTiO_3$ interface.

High-quality $BiFeO_3$ thin films were epitaxially grown on 0.7 wt. % Nb doped (001) $SrTiO_3$ (NSTO) single-crystal substrates by pulsed laser deposition using a KrF excimer laser (248 nm, Lambda Physik COMPex 205) at a frequency of 1 Hz. During the deposition, the substrate temperature was kept at 670 °C, and the oxygen partial pressure was 15 Pa. After deposition, the samples were cooled to room temperature at 4 °C/min in an oxygen pressure of 1 atm. The thickness of BFO film is about 60 nm. The structure of BFO films grown on NSTO substrates was analyzed by x-ray diffraction (XRD, Bruker D8 Advance plus pole figure

[a)]Present address: Energy System Division, Argonne National Laboratory, Argonne, Illinois 60439, USA.
[b)]Author to whom correspondence should be addressed. Electronic mail: myli@whu.edu.cn.

attachment) with Cu K_α radiation. To form Pt/BFO/NSTO heterostructure and measure the electrical properties, Pt top electrodes with diameters of 100, 200, 250, and 750 μm were deposited by dc magnetron sputtering, and In bottom electrode was smeared onto the back of NSTO substrate to ensure Ohmic contact. The current-voltage (I-V) characteristics were performed by a Keithley 4200 semiconductor characterization system with voltage sweeping mode. During the measurement, forward bias was defined as a positive dc voltage applied on the Pt top electrodes. The local piezoresponse and conduction properties were investigated via piezoresponse force microscope (PFM) and conductive atomic force microscopy (C-AFM) on a commercial AFM system (Cypher, Asylum Research) integrated with a Keithley 6517b electrometer, using Pt-coated Si probes (ElectriMulti 75, Budget Sensors). All measurements were carried out at room temperature.

θ-2θ scan in Fig. 1(a) shows that the BFO film is uniformly *c*-axis oriented. The φ-scan of the (011) plane confirms the epitaxial growth of BFO on NSTO substrate, with orientation relationships of BFO(001)/NSTO(001) (out-of-plane) and [110]BFO||[110]NSTO (in-plane), respectively, as shown in the inset of Fig. 1(a). Typical *I-V* characteristics of Pt/BFO/NSTO heterostructure at room temperature are shown in Fig. 1(b). The *I-V* curve exhibits a hysteresis behavior and an asymmetric feature (shown in the inset of Fig. 1(b)), which are corresponding to the resistive switching and the rectifying effect, respectively.[12,18] Electroforming process is not needed to obtain stable resistive switching in our device, indicating that the observed resistive switching comes from interfacial effects rather than conductive filaments.[12] Since BFO is generally considered as a *p*-type semiconductor and NSTO is a *n*-type semiconductor, a Schottky junction and a *p-n* junction are expected to form at the Pt/BFO interface and the BFO/*n*-type semiconductor interface, respectively. Thus, the electrical responses of the Pt/BFO/NSTO heterostructure should be interpreted as a series connection of a reverse and a forward diode. However, the observed forward rectifying behavior in the inset of Fig. 1(b) reveals that the *p-n* junction at BFO/NSTO interface dominates the transport properties of Pt/BFO/NSTO/In heterostructure, while the Schottky barrier at Pt/BFO interface is negligible, which is consistent with the prior reports.[12,16,19]

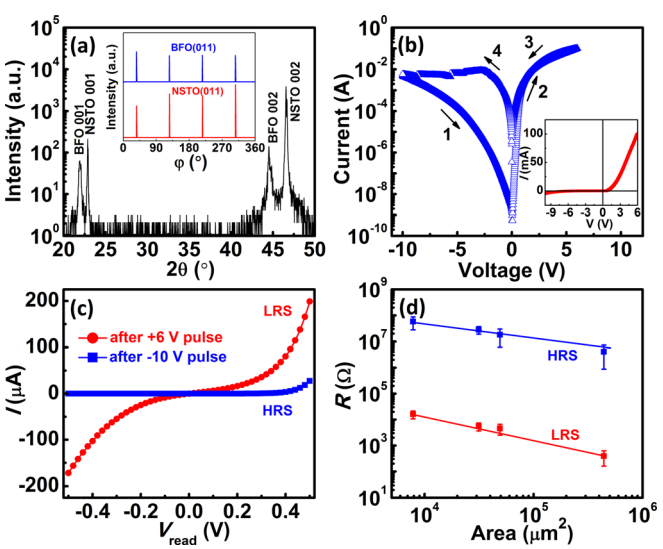

FIG. 1. (a) XRD θ-2θ scan of the BFO/NSTO heterostructure, the inset is φ-scan of the (011) plane; (b) Resistive switching behavior, the inset shows rectifying current-voltage (I-V) characteristics; (c) I-V curves under small reading voltage ($-0.5 \sim +0.5$ V) after applying writing voltage pulses of $+6$ V and -10 V, respectively; (d) Area dependence of the resistances at HRS and LRS.

To investigate the bistable resistive switching in our heterostructure, we applied positive ($+6$ V) and negative (-10 V) pulse voltages (V_{write}) with 1 ms width to polarize the ferroelectric BFO downward and upward, respectively, and then measured the current at low reading voltages V_{read} ($|V_{read}| \leq 0.5\,V \ll |V_{write}|$). These *I-V* curves are shown in Fig. 1(c). Apparently, the current after applying positive V_{write} is higher than that after applying negative V_{write}, which means the resistance switches from HRS (OFF state) to LRS (ON state) when the polarization is reversed from upward to downward. This suggests that the polarization reversal is closely related to the resistive switching in the Pt/BFO/NSTO heterostructure.[11,14] The resistances at both HRS and LRS show strong dependence on the electrode area, as shown in Fig. 1(d). Such area-sensitive resistance behavior indicates that the resistive switching does not correspond to filamentary mechanism.

The as-grown BFO film clearly exhibits randomly polarized ferroelectric domains, and the well-defined, highly reproducible piezoresponse (PR) hysteresis loops are obtained on it, implying a good ferroelectric characteristic of the film, as shown in Figs. 2(a) and 2(b). The marked asymmetry of the PR loops may be in itself related to the rectifying behavior of the BFO/NSTO junction. To examine the correlation between the polarization reversal and the change in electrical conductivity, the polarization in two $1 \times 2\,\mu m^2$ regions has been switched downward and upward by applying bias voltages of $+15$ V and -15 V via the PFM tip, respectively. A current map is then acquired by scanning the poled area with a reading tip bias of -4 V. The results are shown in Figs. 2(c) and 2(d). The area with downward polarization shows significantly higher conductivity than the area upward polarized; in the latter area, no measurable current signals out of the noise floor are present. Note that the lateral size of the conductive areas (up to a few hundred nanometers) in Fig. 2(d) is much larger than that expected for the filaments (typically in tens of nanometers).[20] The local variations in the obtained current map are similar to that recently reported in $BaTiO_3$,[21] which could be ascribed to the film surface roughness, and possibly, to the depth profile of the artificially poled domains that is not assessable with standard PFM capacities, rather than being suggestive of any conductive filaments that are of chemical origins.

Figure 3(a) shows the OFF/ON ratio as a function of reading voltage after applying a 1 ms voltage pulse of $+6$ V or -10 V, respectively. The asymmetry with respect to positive and negative reading voltage should be ascribed to the rectifying effect at the p-n junction.[12] High and stable OFF/ON ratio is observed at negative V_{read}, with OFF/ON ratio of 3000–5000 at -0.2 to -0.5 V, while low OFF/ON ratio of 10–200 is observed at 0.2–0.5 V. This large variation of OFF/ON ratio at different reading voltages could be useful

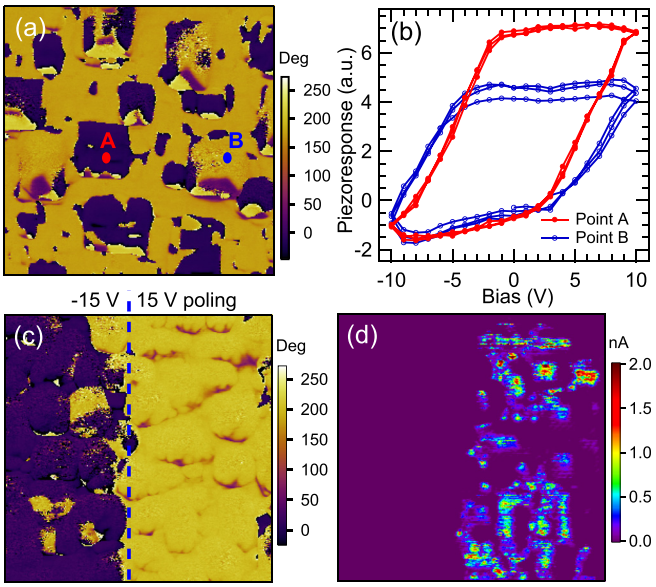

FIG. 2. (a) PFM phase image (out-of-plane) of as-grown BFO film ($1 \times 1\ \mu m^2$); (b) typical piezoresponse hysteresis loops, acquired at two different points as shown in (a); (c) PFM phase image after poling the film using ± 15 V tip bias voltages ($2 \times 2\ \mu m^2$); and (d) Current map acquired in the same region as in (c).

in multistate storage devices. Resistances as a function of writing voltage were measured at $V_{read} = -0.3$ V after applying writing voltage pulses with increasing amplitude, as shown in Fig. 3(b). Since a memristor is a dynamic device depending on pre-history, we applied a reset pulse of $+6$ V or -10 V, respectively, before applying negative or positive writing pulses to avoid a pre-history memory effect.[4] The resistance can be continuously tuned by several orders of magnitude by varying the writing voltage pulse, and the tunability (i.e., R_{OFF}/R_{ON}) reaches $5 \times 10^5\%$ at a writing pulse of -10 V. Furthermore, the hysteretic variation of the resistance with V_{write} is similar to the ferroelectric hysteresis loop, suggesting a ferroelectric polarization modulation of

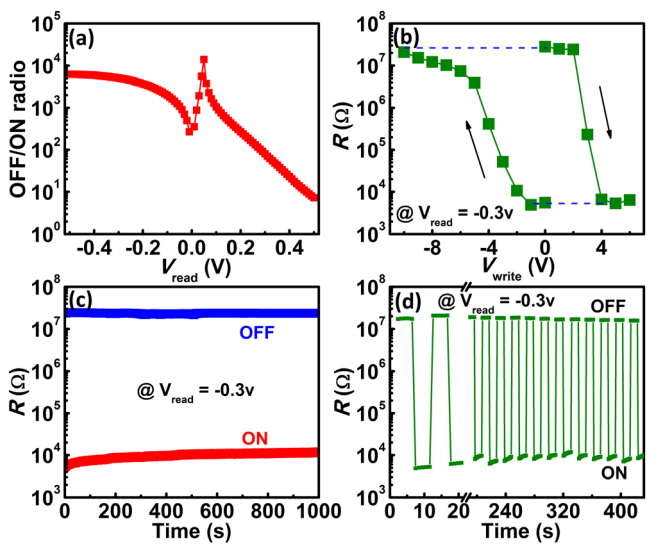

FIG. 3. (a) OFF/ON ratio as a function of reading voltage after applying a 1 ms voltage pulse of $+6$ V and -10 V; (b) Resistance as a function of writing pulse amplitude at $V_{read} = -0.3$ V, showing a continuously tunable memristive behavior; (c) Retention test of OFF and ON states; (d) Fatigue test, revealing the reversible resistance switching between OFF and ON states.

the resistive switching. It is notable that the resistance gradually increases with increasing negative V_{write} and gradually decreases with increasing positive V_{write}, which is opposite to that of the ferroelectric tunnel junctions.[3,4,22] This indicates that a ferroelectric p-n junction effect, rather than a ferroelectric tunneling effect, is responsible for the observed resistive switching behavior in the Pt/BFO/NSTO heterostructure. Retention and fatigue tests were carried out at $V_{read} = -0.3$ V after applying writing voltage pulse of $+6$ V or -10 V to set the ON or OFF states, respectively, as shown in Figs. 3(c) and 3(d). The resistance states are highly stable and reversible, revealing excellent retention and anti-fatigue properties in our ferroelectric resistive switching device.

To investigate the conduction mechanism inside the BFO films, three possible conduction models,[23] i.e., Schottky emission, Poole-Frenkel emission, and space-charge-limited conduction (SCLC), were used to fit the current density-voltage (J-V) curves at LRS. The best fit comes from the SCLC mechanism,[11,24] which is shown in Figs. 4(a) and 4(b). At low V ($|V| \leq 0.2$ V), $\log(|J|)$ initially exhibits linear relationship with $\log(|V|)$ (i.e., $J \propto V$), indicating an Ohmic conduction behavior. With increasing V, nonlinear relationship between $\log(|J|)$ and $\log(|V|)$ is present (i.e., $J \propto V^n$, $n \geq 2$).[11] For HRS, it is difficult to analyze the conduction mechanism inside the BFO films due to the large resistance of p-n junction, which exhibits a typical unilateral conduction behavior.[24] In a semiconductor diode, the reverse current increases slightly with negative voltage and is not completely saturated due to the generation and combination of minority carriers in the depletion region, consistent with our results in Fig. 4(c). On the other hand, the forward current I of an ideal diode can be expressed as

$$I = I_0 \exp\left(\frac{qV}{k_B T}\right), \tag{1}$$

where I_o is the saturated reverse current, q is the charge of electron, k_B is the Boltzmann constant, and T is the absolute temperature. Therefore, for an ideal diode, $\ln I$ should have a

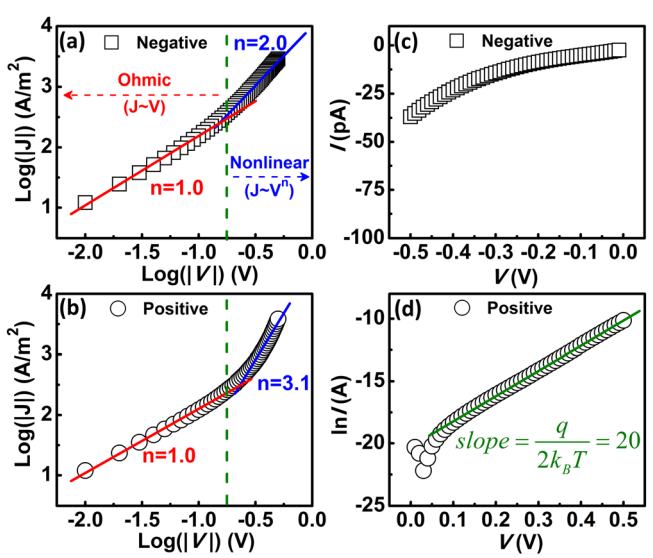

FIG. 4. Conduction mechanisms of (a), (b) LRS, and (c), (d) HRS under negative and positive voltages.

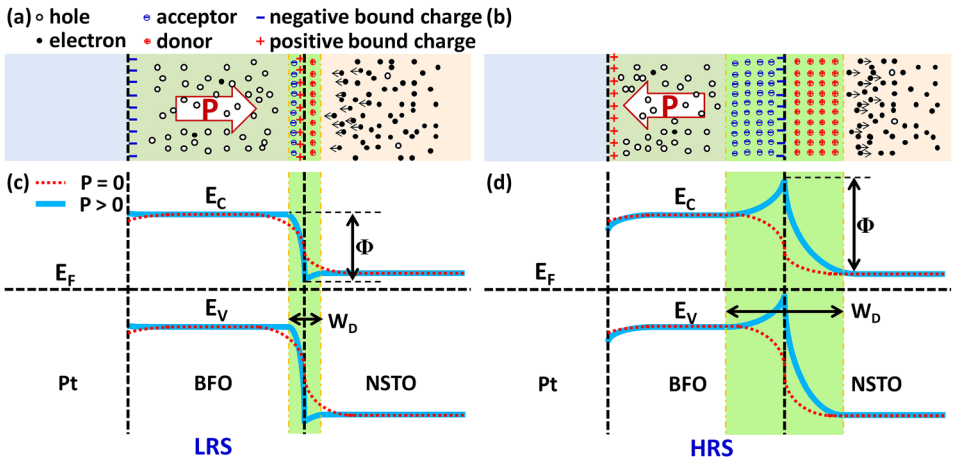

FIG. 5. Schematic (a), (b) charge distribution and (c), (d) energy-band diagrams of the Pt/BFO/NSTO heterostructure at LRS and HRS.

linear plot with V with a slope of q/k_BT. However, for a semiconductor diode, a slope of $q/2k_BT$ is generally observed when the forward current is low,[24] which is also in good agreement with our result, as shown in Fig. 4(d). The analysis of conduction mechanism suggests that SCLC is the responsible conduction route at LRS (downward polarization), while the *p-n* junction conduction is dominant at HRS (upward polarization).

Based on these detailed examinations, the observed resistive switching behavior in the Pt/BFO/NSTO heterostructure can be explained by considering the ferroelectric polarization modulation effect on the width of depletion region and the height of potential barrier at the BFO/NSTO interface.[25,26] Assuming no contribution from the polarization in the as-grown films, a depletion region with a certain width forms across the p-n junction after reaching dynamic equilibrium, as a result of the interdiffusion of majority carriers. The depletion region also induces an energy band bending and a potential barrier at the interface.[24] When the ferroelectric polarization in BFO is downward after applying a large positive writing voltage pulse (+6 V), the positive polarization bound charges aggregate at the BFO/NSTO interface. Through the ferroelectric field effect,[27] the negative majority electron carriers in n-type NSTO are attracted by these positive bound charges and migrate toward the interface, resulting in a decrease in the depletion width, as sketched in Fig. 5(a). In contrast, when the polarization is upward after applying a large negative voltage pulse (−10 V), the negative majority electron carriers in n-type NSTO are repelled by the negative bound charges at the BFO/NSTO interface, which increases the depletion width, as shown in Fig. 5(b). Furthermore, since the screening of the bound charges is usually incomplete, a depolarization field with opposite direction to the polarization is developed in the ferroelectric layer[28] and consequently leads to energy band bending at the interface,[25] as shown in the band diagram of Pt/BFO/NSTO heterostructure in Figs. 5(c) and 5(d). The total potential barrier after applying positive pulse is lower than that after applying negative pulse.[12] Therefore, the carriers can readily pass through the depletion region under an electric field after applying +6 V pulse, due to the relatively narrow depletion region and low potential barrier height at the p-n junction.[24] The device is then set to a stable low resistance state. After that, if negative voltage pulses with increasing amplitude are consecutively applied, the depletion width and barrier height will gradually increase due to the increasing upward polarization, resulting in a continuously increasing resistance. Conversely, if the device is initially set to HRS by upward polarization and then positive pulses are applied, the resistance continuously decreases with increasing positive voltage amplitude. Therefore, the memristive behavior in Pt/BFO/NSTO heterostructure could be attributed to the modulation effect of ferroelectric polarization on both the depletion width and the potential barrier height of the BFO/NSTO *p-n* junction.

In summary, epitaxial ferroelectric BFO films were prepared by pulsed laser deposition on Nb-doped $SrTiO_3$ substrates. A memristive resistive switching behavior with a continuous tunability up to $5 \times 10^5\%$ and excellent retention and anti-fatigue characteristics was observed in Pt/BFO/NSTO heterostructure, which is attributed to the ferroelectric polarization modulation of the depletion width and the potential barrier height of the BFO/NSTO interface. This ferroelectric memristor extends the functionality of BFO-based heterostructures and has potential application in nonvolatile memories and logic devices.

This work was supported by the National Natural Science Foundation of China (Grant Nos. 11074193 and 51132001). Q.L. and Y.L. acknowledge the support of the Australian Research Council (ARC) in the form of ARC Discovery Grants.

[1]D. S. Jeong, R. Thomas, R. S. Katiyar, J. F. Scott, H. Kohlstedt, A. Petraru, and C. S. Hwang, Rep. Prog. Phys. **75**, 076502 (2012).
[2]C. H. Yang, J. Seidel, S. Y. Kim, P. B. Rossen, P. Yu, M. Gajek, Y. H. Chu, L. W. Martin, M. B. Holcomb, Q. He, P. Maksymovych, N. Balke, S. V. Kalinin, A. P. Baddorf, S. R. Basu, M. L. Scullin, and R. Ramesh, Nature Mater. **8**(6), 485–493 (2009).
[3]A. Chanthbouala, V. Garcia, R. O. Cherifi, K. Bouzehouane, S. Fusil, X. Moya, S. Xavier, H. Yamada, C. Deranlot, N. D. Mathur, M. Bibes, A. Barthélémy, and J. Grollier, Nature Mater. **11**(10), 860–864 (2012).
[4]D. J. Kim, H. Lu, S. Ryu, C. W. Bark, C. B. Eom, E. Y. Tsymbal, and A. Gruverman, Nano Lett. **12**(11), 5697–5702 (2012).
[5]D. B. Strukov, G. S. Snider, D. R. Stewart, and R. S. Williams, Nature **453**(7191), 80–83 (2008).
[6]S.-W. Chen and J.-M. Wu, Thin Solid Films **519**(1), 499–504 (2010).
[7]X. Chen, G. Wu, H. Zhang, N. Qin, T. Wang, F. Wang, W. Shi, and D. Bao, Appl. Phys. A **100**(4), 987–990 (2010).
[8]K. Yin, M. Li, Y. Liu, C. He, F. Zhuge, B. Chen, W. Lu, X. Pan, and R.-W. Li, Appl. Phys. Lett. **97**(4), 042101 (2010).

[9]Z. Hu, M. Li, Y. Zhu, S. Pu, X. Liu, B. Sebo, X. Zhao, and S. Dong, Appl. Phys. Lett. **100**(25), 252908 (2012).
[10]A. Q. Jiang, C. Wang, K. J. Jin, X. B. Liu, J. F. Scott, C. S. Hwang, T. A. Tang, H. B. Lu, and G. Z. Yang, Adv. Mater. **23**(10), 1277–1281 (2011).
[11]D. Lee, S. H. Baek, T. H. Kim, J. G. Yoon, C. M. Folkman, C. B. Eom, and T. W. Noh, Phys. Rev. B **84**(12), 125305 (2011).
[12]T. L. Qu, Y. G. Zhao, D. Xie, J. P. Shi, Q. P. Chen, and T. L. Ren, Appl. Phys. Lett. **98**(17), 173507 (2011).
[13]C. Wang, K.-J. Jin, Z.-T. Xu, L. Wang, C. Ge, H.-B. Lu, H.-Z. Guo, M. He, and G.-Z. Yang, Appl. Phys. Lett. **98**(19), 192901 (2011).
[14]A. Tsurumaki, H. Yamada, and A. Sawa, Adv. Funct. Mater. **22**(5), 1040–1047 (2012).
[15]G. I. Meijer, Science **319**(5870), 1625–1626 (2008).
[16]H. Yang, H. M. Luo, H. Wang, I. O. Usov, N. A. Suvorova, M. Jain, D. M. Feldmann, P. C. Dowden, R. F. DePaula, and Q. X. Jia, Appl. Phys. Lett. **92**(10), 102113 (2008).
[17]Y. Watanabe, Ferroelectrics **349**(1), 190–209 (2007).
[18]S. Y. Yang, L. W. Martin, S. J. Byrnes, T. E. Conry, S. R. Basu, D. Paran, L. Reichertz, J. Ihlefeld, C. Adamo, A. Melville, Y. H. Chu, C. H. Yang, J. L. Musfeldt, D. G. Schlom, J. W. Ager, and R. Ramesh, Appl. Phys. Lett. **95**(6), 062909 (2009).
[19]H. Khassaf, G. A. Ibanescu, I. Pintilie, I. B. Misirlioglu, and L. Pintilie, Appl. Phys. Lett. **100**(25), 252903 (2012).
[20]D.-H. Kwon, K. M. Kim, J. H. Jang, J. M. Jeon, M. H. Lee, G. H. Kim, X.-S. Li, G.-S. Park, B. Lee, S. Han, M. Kim, and C. S. Hwang, Nat. Nanotechnol. **5**(2), 148–153 (2010).
[21]G. Kim, D. Mazumdar, and A. Gupta, Appl. Phys. Lett. **102**(5), 052908 (2013).
[22]A. Chanthbouala, A. Crassous, V. Garcia, K. Bouzehouane, S. Fusil, X. Moya, J. Allibe, B. Dlubak, J. Grollier, S. Xavier, C. Deranlot, A. Moshar, R. Proksch, N. D. Mathur, M. Bibes, and A. Barthelemy, Nat. Nanotechnol. **7**(2), 101–104 (2012).
[23]G. W. Pabst, L. W. Martin, Y.-H. Chu, and R. Ramesh, Appl. Phys. Lett. **90**(7), 072902 (2007).
[24]S. M. Sze and K. K. Ng, *Physics of Semiconductor Devices* (Wiley-Interscience, Hoboken, 2007).
[25]Y. Watanabe, Phys. Rev. B **59**(17), 11257 (1999).
[26]R. Meyer and R. Waser, J. Appl. Phys. **100**(5), 051611 (2006).
[27]S. Mathews, R. Ramesh, T. Venkatesan, and J. Benedetto, Science **276**(5310), 238–240 (1997).
[28]R. R. Mehta, B. D. Silverman, and J. T. Jacobs, J. Appl. Phys. **44**(8), 3379–3385 (1973).